

**PETROLOGY AND GEOCHEMISTRY OF ERRACHIDIA 004, A POLYMICT WINONAITE  
COMPOSED OF DISTINCT HIGH AND LOW METAL LITHOLOGIES.**

D. Sheikh<sup>1</sup>, <sup>1</sup>Cascadia Meteorite Laboratory, Portland State University, Department of Geology, Portland, OR 97207, USA, email: dsheikh@pdx.edu

**Introduction:** Errachidia 004 is a recently recovered meteorite from Morocco in 2020 with a total mass of 2.64 kg. Most of the recovered fragments were only a few grams in mass, and it was noted that ~75% of the recovered fragments displayed low amounts of visible Fe-Ni metal while the remaining ~25% displayed high amounts of visible Fe-Ni metal. Multiple fragments were provided for classification by Sean Mahoney, of which two thin sections were made, one from a high metal fragment and one from a low metal fragment.

**Petrology:** Errachidia 004 exhibits two distinct lithologies (Fig. 1): 1) A low-metal lithology displaying a predominantly granoblastic texture composed of forsterite, enstatite, augite, and accessory sodic plagioclase (silicate grain size Av. 160  $\mu\text{m}$ ) with grain boundaries meeting at approximately 120° triple junctions. Troilite and accessory kamacite are finely scattered throughout the interior as either veinlets or individual grains; some have been altered to form Fe-oxides. 2) A high-metal lithology (up to 80 vol. % metal) displaying a well-developed Widmanstätten pattern containing kamacite, taenite, and accessory troilite and schreibersite (kamacite band width Av. 2 mm), and containing angular to sub-rounded grains of sodic plagioclase (some containing melt inclusions), augite, enstatite, and accessory Si-Al-rich glass (silicate grain size Av. 400  $\mu\text{m}$ ). No chondrules were observed in either lithology.

**Geochemistry:** Major and minor element data obtained via EPMA at FIU of the silicate phases in both lithologies is displayed in Table 1. No noticeable differences are observed between low-Ca pyroxene, high-Ca pyroxene, and plagioclase grains present in both the high and low metal lithologies. Oxygen isotopic data obtained via laser fluorination at UNM of both high and low metal lithologies are displayed (Fig. 2) and plot within the field for winonaite [1]. Siderophile element concentrations obtained via ICP-MS at UAlberta of a metal-separate from the high-metal lithology are reported: Ni 7.4, Co 0.30 (both reported in wt. %), Ir 5.9, Ga 28, Ge 123, As 10.1, Ru 5.0, Re 0.5, Os 13.6, Pt 9.5, Cu 180, Au 1.51 (reported in ppm). This composition would be placed into the IAB field [2].

**Discussion:** The textural, chemical, and isotopic characteristics of Errachidia 004 indicate that this meteorite is a winonaite [1, 3]. The co-existence of two distinct lithologies within this polymict winonaite: 1) metal-depleted ultramafic melt residue, and 2) silicate-rich IAB of basaltic composition, requires for breakup and re-assembly of the winonaite-IAB parent body [4-5] to have occurred at a small enough scale for multiple lithologies from various depths to be mixed into meter-sized objects and subsequently thermally metamorphosed, i.e. a rubble pile.

**References:** [1] Greenwood et al. (2012) *Geochimica et Cosmochimica Acta* 94:146-163. [2] Wasson and Kallemeyn (2002) *Geochimica et Cosmochimica Acta* 66:2445-2473. [3] Benedix et al. (1998) *Geochimica et Cosmochimica Acta* 62:2535-2553. [4] Benedix et al. (2000) *Meteoritics & Planetary Science* 35:1127-1141. [5] Zeng et al. (2019) *Earth, Planets and Space* 71:38.

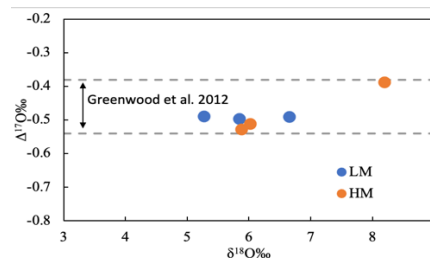
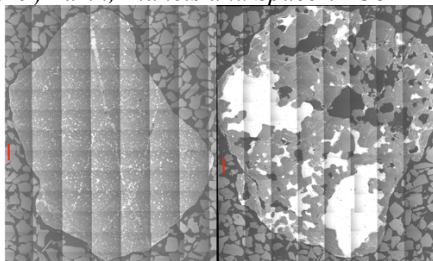


Fig. 1. BSE mosaics of low (left) and high (right) metal lithologies. Fig. 2. O-isotopes of both lithologies.

**Table 1. Representative Microprobe Data from Silicate Phases in High and Low Metal Lithologies**

	Olivine-LM	Low-Ca Pyroxene-LM	High-Ca Pyroxene-LM	Plagioclase-LM	Low-Ca Pyroxene-HM	High-Ca Pyroxene-HM	Plagioclase-HM
wt. %	n=23	n=21	n=8	n=2	n=3	n=23	n=16
MgO	53.8 (0.4)	37.4 (0.5)	18.8 (0.3)	b.d.l.	34.4 (0.6)	17.6 (0.6)	b.d.l.
SiO <sub>2</sub>	43.7 (0.8)	57.2 (0.7)	53.2 (0.8)	65.0 (0.8)	59.1 (0.8)	54.6 (0.9)	63.8 (0.9)
FeO	0.85 (0.29)	3.51 (0.40)	1.63 (0.93)	0.13 (0.11)	3.52 (0.18)	1.46 (0.14)	0.05 (0.04)
Na <sub>2</sub> O	b.d.l.	b.d.l.	0.95 (0.09)	10.40 (0.30)	b.d.l.	0.99 (0.05)	10.03 (0.67)
Cr <sub>2</sub> O <sub>3</sub>	b.d.l.	0.26 (0.05)	1.44 (0.24)	b.d.l.	0.33 (0.07)	1.65 (0.09)	b.d.l.
Al <sub>2</sub> O <sub>3</sub>	b.d.l.	0.42 (0.07)	1.31 (0.13)	21.54 (0.30)	0.48 (0.06)	1.33 (0.08)	22.32 (0.44)
K <sub>2</sub> O	b.d.l.	b.d.l.	b.d.l.	1.03 (0.13)	b.d.l.	b.d.l.	0.87 (0.10)
TiO <sub>2</sub>	b.d.l.	0.21 (0.07)	0.75 (0.10)	b.d.l.	0.14 (0.09)	0.79 (0.15)	0.09 (0.06)
MnO	0.33 (0.17)	0.77 (0.09)	0.45 (0.03)	b.d.l.	0.72 (0.11)	0.48 (0.05)	b.d.l.
CaO	b.d.l.	0.90 (0.15)	21.86 (0.67)	2.16 (0.02)	1.03 (0.24)	21.39 (0.79)	2.47 (0.35)
Total	98.7 (0.9)	100.7 (0.6)	100.4 (0.9)	100.3 (0.9)	99.7 (2.1)	100.3 (1.0)	99.6 (0.9)
Fa	0.9 (0.3)	-	-	-	-	-	-
Fs	-	4.9 (0.6)	2.6 (1.4)	-	5.3 (0.2)	2.4 (0.2)	-
Wo	-	1.6 (0.3)	44.4 (1.3)	-	2.0 (0.4)	45.5 (1.6)	-
An	-	-	-	9.7 (0.3)	-	-	11.1 (1.6)
Or	-	-	-	5.5 (0.8)	-	-	4.8 (0.5)

LM- low metal, HM- high metal, b.d.l.- below detection limit, standard deviation in parenthesis.